phenol red or riboflavins and supplemented with 25 mM HEPES and 0.2% BSA. Solutions were maintained at 4 °C until immediately before each experiment, when they were warmed to 37 °C and supplemented with 50 nM PdBU and either 0.5 mM EGTA (~50 μM free Ca^{2+}) or 1 mM Ca^{2+} (1.5 mM total Ca^{2+}).

Transfection of the reporter genes. NF-AT, NF-κB, Oct-1/OAP and IL-2 reporter constructs were provided by J. Goldberg and G. Crabtree and were derived from constructs described previously[16]. Multimeric copies of NFAT (3 copies), NF-κB (4) or Oct/Oap (4) binding sites, linked to a minimal (non-inducible) IL-2 promoter (−74 to +47), were inserted between the *Sma*I and *Hin*dIII sites in the multiple cloning region of the pGL-3 luciferase reporter vector (Promega). The construct with the intact IL-2 promoter region was made by inserting 371 bp of the IL-2 initiation region (−324 to +47) into the pGL-3 vector. The IL-8 reporter construct was provided by K. P. LeClair[27].

Transfection of 10^7 cells was by electroporation with 10 μg of the reporter vector, 1 μg of a vector containing large-T antigen and 2 μg of a vector encoding the transmembrane and extracellular domains of CD8. Large-T antigen was used to increase the number of copies of the reporter construct in each cell, and the CD8 construct was used to determine the transfection efficiency. Transfection efficiencies were 30–40%; viability following centrifugation to remove cells killed during electroporation was 85–95%. Experiments were conducted 24–48 h after transfection when the expression of reporter genes was maximal.

Ca^{2+} clamp and Ca^{2+} measurements. Transfected cells were loaded with 2 μM Fura-PE3/AM (Teflabs) for 1 h at 37 °C in loading medium (RPMI 1640, 25 mM HEPES, 2% fetal bovine serum), washed, and incubated for another hour to allow complete de-esterification of the dye. Loaded cells ($2–3 \times 10^5$) were allowed to adhere to a polylysine-coated laminar flow chamber and were placed on the heated stage of a Zeiss Axiovert 35 inverted microscope. The laminar flow chamber (60 μl volume) was connected to two heated reservoirs containing 1.5 mM and 0 mM Ca^{2+} solutions, and pressurized with a mixture of 95% air and 5% CO_2. At the start of each experiment, cells were treated with 1 μM thapsigargin in 0 mM Ca^{2+} solution for 5 min to deplete internal Ca^{2+} stores and irreversibly activate CRAC channels. A computer-controlled solenoid valve (General Valve) was used to switch rapidly between the Ca^{2+}-containing and Ca^{2+}-free solutions flowing into the chamber and over the cells. The solution in the chamber was fully exchanged about once per second and was maintained at 37 °C. Cells were stimulated for 3 h while $[Ca^{2+}]_i$ was measured every 5–10 s by video microscopy as described[10]. Fura-PE3 was calibrated on the microscope in a microcuvette using solutions containing 1 mM EGTA and 10 mM Ca^{2+} according to ref. 10.

Reporter gene assays. Following stimulation cells were washed from the chamber, lysed by freeze/thawing and subjected to a luciferase assay using standard methods. All measurements were done in triplicate and normalized to the total number of cells determined using a Coulter Counter (Coulter Electronics). β-Galactosidase (β-gal) expression was measured by flow cytometry using the FACS–Gal protocol[13]. Steady-state $[Ca^{2+}]_i$ dependence of luciferase reporter genes (Fig. 3) was determined after 3 h stimulation with 1 μM thapsigargin, 50 nM PdBU and variable extracellular $[Ca^{2+}]$. Luciferase activity was normalized to values between 0 and 100%, given by the responses to TG + PdBU in medium containing 0.5 mM EGTA or 1.5 mM Ca^{2+}, respectively.

Received 16 December 1997; accepted 12 February 1998.

1. Berridge, M. J. & Galione, A. Cytosolic calcium oscillators. *FASEB J.* **2,** 3074–3082 (1988).
2. Tsien, R. W. & Tsien, R. Y. Calcium channels, stores, and oscillations. *Annu. Rev. Cell Biol.* **6,** 715–760 (1990).
3. Fewtrell, C. Ca^{2+} oscillations in non-excitable cells. *Annu. Rev. Physiol.* **55,** 427–454 (1993).
4. Thomas, A. P., Bird, G. S. J., Hajnóczky, G., Robb-Gaspers, L. D. & Putney, J. W. Jr Spatial and temporal aspects of cellular calcium signaling. *FASEB J.* **10,** 1505–1517 (1996).
5. Negulescu, P. A., Shastri, N. & Cahalan, M. D. Intracellular calcium dependence of gene expression in single T lymphocytes. *Proc. Natl Acad. Sci. USA* **91,** 2873–2877 (1994).
6. Dolmetsch, R. E. & Lewis, R. S. in *Imaging Living Cells: A Laboratory Manual* (eds Konnerth, A., Lanni, F. & Yuste, R.) (CSHL Press, Cold Spring Harbor, in the press).
7. Lewis, R. S. & Cahalan, M. D. Potassium and calcium channels in lymphocytes. *Annu. Rev. Immunol.* **13,** 623–653 (1995).
8. Zweifach, A. & Lewis, R. S. Mitogen-regulated Ca^{2+} current of T lymphocytes is activated by depletion of intracellular Ca^{2+} stores. *Proc. Natl Acad. Sci. USA* **90,** 6295–6299 (1993).
9. Lewis, R. S. & Cahalan, M. D. Mitogen-induced oscillations of cytosolic Ca^{2+} and transmembrane Ca^{2+} current in human leukemic T cells. *Cell Reg.* **1,** 99–112 (1989).
10. Dolmetsch, R. & Lewis, R. S. Signaling between intracellular Ca^{2+} stores and depletion-activated Ca^{2+} channels generates $[Ca^{2+}]_i$ oscillations in T lymphocytes. *J. Gen. Physiol.* **103,** 365–388 (1994).
11. Crabtree, G. R. & Clipstone, N. A. Signal transmission between the plasma membrane and nucleus of T lymphocytes. *Annu. Rev. Biochem.* **63,** 1045–1083 (1994).
12. Rao, A. NF-ATp: a transcription factor required for the coordinate induction of several cytokine genes. *Immunol. Today* **15,** 274–281 (1994).
13. Fiering, S. *et al.* Single cell assay of a transcription factor reveals a threshold in transcription activated by signals emanating from the T-cell antigen receptor. *Genes Dev.* **4,** 1823–1834 (1990).
14. Donnadieu, E. *et al.* Imaging early steps of human T cell activation by antigen-presenting cells. *J. Immunol.* **148,** 2643–2653 (1992).
15. Frantz, B. *et al.* Calcineurin acts in synergy with PMA to inactivate IκB/MAD3, an inhibitor of NF-κB. *EMBO J.* **13,** 861–870 (1994).
16. Mattila, P. S. *et al.* The actions of cyclosporin A and FK506 suggest a novel step in the activation of T lymphocytes. *EMBO J.* **9,** 4425–4433 (1990).
17. Baeuerle, P. A. & Henkel, T. Function and activation of NF-κB in the immune system. *Annu. Rev. Immunol.* **12,** 141–179 (1994).
18. Clipstone, N. A. & Crabtree, G. R. Identification of calcineurin as a key signalling enzyme in T-lymphocyte activation. *Nature* **357,** 695–697 (1992).
19. Liu, J. *et al.* Calcineurin is a common target of cyclophilin-cyclosporin A and FKBP-FK506 complexes. *Cell* **66,** 807–815 (1991).
20. Fanger, C. M., Hoth, M., Crabtree, G. R. & Lewis, R. S. Characterization of T cell mutants with defects in capacitative calcium entry: Genetic evidence for the physiological roles of CRAC channels. *J. Cell Biol.* **131,** 655–667 (1995).
21. Dolmetsch, R. E., Lewis, R. S., Goodnow, C. C. & Healy, J. I. Differential activation of transcription factors induced by Ca^{2+} response amplitude and duration. *Nature* **386,** 855–858 (1997).
22. Li, W.-h., Llopis, J., Whitney, M., Zlokarnik, G. & Tsien, R. Y. Cell-permeant caged $InsP_3$ ester shows that Ca^{2+} spike frequency can optimize gene expression. *Nature* **392,** 936–941 (1998).
23. Shibasaki, F., Price, E., Milan, D. & McKeon, F. Role of kinases and the phosphatase calcineurin in the nuclear shuttling of transcription factor NF-AT4. *Nature* **382,** 370–373 (1996).
24. Durand, D. B., Bush, M. R., Morgan, J. G., Weiss, A. & Crabtree, G. R. A 275 base pair fragment at the 5′ end of the interleukin 2 gene enhances expression from a heterologous promoter in response to signals from the T cell antigen receptor. *J. Exp. Med.* **165,** 395–407 (1987).
25. Okamoto, S. *et al.* The interleukin-8 AP-1 and κB-like sites are genetic end targets of FK506-sensitive pathway accompanied by calcium mobilization. *J. Biol. Chem.* **269,** 8582–8589 (1994).
26. Durand, D. B. *et al.* Characterization of antigen receptor response elements within the interleukin-2 enhancer. *Mol. Cell. Biol.* **8,** 1715–1724 (1988).
27. Wechsler, A. S., Gordon, M. C., Dendorfer, U. & LeClair, K. P. Induction of IL-8 expression in T cells uses the CD28 costimulatory pathway. *J. Immunol.* **153,** 2515–2523 (1994).
28. Prussin, C. & Metcalfe, D. D. Detection of intracytoplasmic cytokine using flow cytometry and directly conjugated anti-cytokine antibodies. *J. Immunol. Meth.* **188,** 117–128 (1995).
29. Gu, X. & Spitzer, N. C. Distinct aspects of neuronal differentiation encoded by frequency of spontaneous Ca^{2+} transients. *Nature* **375,** 784–787 (1995).
30. Fields, R. D., Eshete, F., Stevens, B. & Itoh, K. Action potential-dependent regulation of gene expression: temporal specificity in Ca^{2+}, cAMP-responsive element binding proteins, and mitogen-activated protein kinase signaling. *J. Neurosci.* **17,** 7252–7266 (1997).

Acknowledgements. We thank J. Goldberg for NF-AT-, Oct/OAP- and NF-κB-luciferase constructs; K. LeClair and G. Crabtree for IL-8 and IL-2 luciferase constructs; C. Fanger for creating the large T antigen and CD8 constructs; G. Crabtree and L. Herzenberg for use of the luminometer and electroporator; S. Finkbeiner, Y. Gotoh and M. Greenberg for comments on the manuscript; and J. Walton for help in preparing constructs. This work was supported by a grant from the NIH (R.S.L.) and by a predoctoral fellowship from the American Heart Association, California Affiliate (R.E.D.).

Correspondence and requests for materials should be addressed to R.S.L. (e-mail: rslewis@leland.stanford.edu).

Cell-permeant caged $InsP_3$ ester shows that Ca^{2+} spike frequency can optimize gene expression

Wen-hong Li*†‡, Juan Llopis*, Michael Whitney§, Gregor Zlokarnik§ & Roger Y. Tsien*†¶

*Departments of * Pharmacology and † Chemistry & Biochemistry, and ¶ Howard Hughes Medical Institute, University of California, San Diego, 9500 Gilman Drive, La Jolla, California 92093-0647, USA*
§ Aurora Biosciences Corporation, 11010 Torreyana Road, San Diego, California 92121, USA

Inositol 1,4,5-trisphosphate ($InsP_3$) releases calcium from intracellular stores and triggers complex waves and oscillations in levels of cytosolic free calcium[1–5]. To determine which longer-term responses are controlled by oscillations in $InsP_3$ and cytosolic free calcium, it would be useful to deliver exogenous $InsP_3$, under spatial and temporal control, into populations of unpermeabilized cells. Here we report the 15-step synthesis of a

‡ Present address: Division of Biology 139-74, Beckman Institute, California Institute of Technology, Pasadena, California 91125, USA.

membrane-permeant, caged $InsP_3$ derivative from *myo*-inositol. This derivative diffused into intact cells and was hydrolysed to produce a caged, metabolically stable $InsP_3$ derivative. This latter derivative accumulated in the cytosol at concentrations of hundreds of micromolar, without activating the $InsP_3$ receptor. Ultraviolet illumination uncaged an $InsP_3$ analogue nearly as potent as real $InsP_3$, and generated spikes of cytosolic free calcium, and stimulated gene expression via the nuclear factor of activated T cells[6,7]. The same total amount of $InsP_3$ analogue elicited much more gene expression when released by repetitive flashes at 1-minute intervals than when released at 0.5- or ⩾2-minute intervals, as a single pulse, or as a slow sustained plateau. Thus, oscillations in cytosolic free calcium levels at roughly physiological rates maximize gene expression for a given amount of $InsP_3$.

The physiological functions of oscillations in cytosolic free calcium ($[Ca^{2+}]_c$) levels and the existence of $InsP_3$ oscillations remain controversial[1–4]. Stimulation with natural agonists does not allow dissection of the relative contributions of oscillation amplitude, frequency, number of pulses, and branching transduction pathways involving, for example, receptor tyrosine kinase activity or diacylglycerol production. It would be preferable to impose oscillations of various frequencies and a steady non-oscillatory elevation, and to compare their efficacies in triggering downstream events such as secretion or gene activation. One could drive $[Ca^{2+}]_c$ signals with either $InsP_3$ or extracellular Ca^{2+}; the latter strategy[8] also requires elevating the permeability of the plasma membrane to Ca^{2+}. We chose to use $InsP_3$ pulses because they mimic the natural cycle of calcium release from internal stores, work

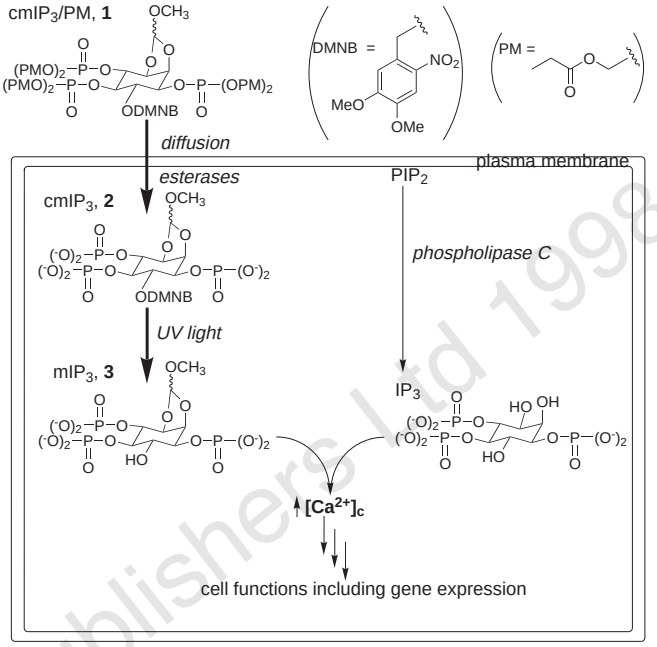

Figure 1 Mode of action of the caged, membrane-permeant $InsP_3$ derivative cmInsP_3/PM (cmIP$_3$/PM) (compound **1**), the trapped caged molecule (cmInsP_3 (cmIP$_3$), compound **2**), and 2,3-methoxymethylene-InsP_3 (mInsP_3, compound **3**) released by photolysis. PM, propionyloxymethyl group; DMNB, 4,5-dimethoxy-2-nitrobenzyl group.

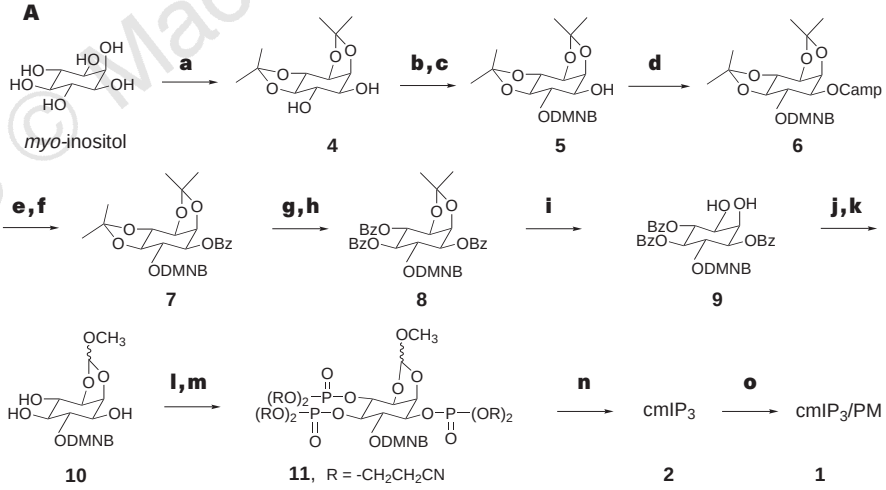

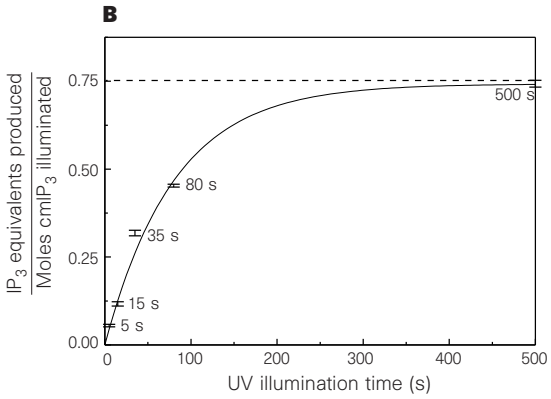

Figure 2 Synthesis and biochemical characterization of cmInsP_3/PM and its reaction products. **A**, Chiral synthesis of cmInsP_3/PM, starting from *myo*-inositol. Bz, benzoyl; Camp, *S*-camphanyl. Reagents: **a**, 2-methoxypropene in acidic dimethylformamide (DMF), followed by chromatography and crystallization[26]; **b**, Bu_2SnO, toluene azeotropy, 63% yield; **c**, DMNB bromide, CsF, DMF; **d**, S-(–)-camphanic acid chloride, triethylamine, 4-dimethylaminopyridine, then silica gel chromatography and crystallization to separate the diastereomeric camphanates, 42% of the desired isomer; **e**, K_2CO_3, methanol/CH_2Cl_2; **f**, BzCl, pyridine, 80%; **g**, $HSCH_2CH_2OH$, BF_3/Et_2O; **h**, BzCl, pyridine, 76%; **i**, $HSCH_2CH_2OH$, BF_3/Et_2O, 80%; **j**, $HC(OMe)_3$, BF_3/Et_2O, DMF; **k**, K_2CO_3, methanol/CH_2Cl_2, 52%; **l**, $(NCCH_2CH_2O)_2PN(i\text{-}Pr_2$, tetrazole; **m**, t-butyl hydroperoxide, CH_2Cl_2, 79%; **n**, NH_3, aqueous methanol; **o**, $EtCOOCH_2Br$, $(i\text{-}Pr)_2NEt$, CH_3CN, 12% for steps **n** + **o**. **B**, Binding to the $InsP_3R$, measured as equivalent picomol of genuine $InsP_3$ (IP_3), as a function of duration of ultraviolet-light-mediated photolysis of 8-pmol aliquots of cminsP$_3$ (cmIP$_3$) *in vitro*. The smooth curve and dashed line show the fitted exponential progress curve (see Methods) and its asymptote, respectively.

at normal extracellular calcium levels, incorporate the complex relationship between $InsP_3$ and $[Ca^{2+}]_c$, and may be useful for many other studies.

Standard techniques for delivering the highly charged $InsP_3$ molecule across cell membranes, such as membrane permeabilization, microinjection, or patch clamping, would not allow reliable measurement of subsequent complex events, such as gene expression, in enough cells. To achieve precise temporal control without disrupting the plasma membrane, we needed a membrane-permeant derivative of caged $InsP_3$, such as $cmInsP_3$/PM (compound **1** in Fig. 1). All three phosphates of this compound were esterified with propionyloxymethyl (PM) groups, which hydrolyse in the cytoplasm to produce $cmInsP_3$ (compound **2** in Fig. 1). Free 2- and 3-hydroxyl groups are not obligatory[9–11] for binding to the $InsP_3$ receptor ($InsP_3R$), so we masked these groups with a methoxymethylene group, which is relatively small and should not interfere with binding to the $InsP_3R$. Blockage of the 3-hydroxyl should prevent the released $InsP_3$ analogue from being phosphorylated by $InsP_3$ 3-kinase to inositol 1,3,4,5-tetrakisphosphate. The 6-hydroxyl of $InsP_3$ interacts specifically with the $InsP_3R$ and is essential[10,11] for release of calcium, yet is difficult to regenerate from a permeant ester, perhaps because the bulky flanking 1- and 5-phosphate groups hinder the hydrolysis[12]. Therefore we protected the 6-hydroxyl with a photolabile caging group, a 4,5-dimethoxy-2-nitrobenzyl (DMNB) ether[13]. Ultraviolet-mediated photolysis of the DMNB group should be independent of steric shielding by the flanking phosphates and should abruptly switch on biological activity through formation of compound **3** (2,3-methoxymethylene-$InsP_3$, or $mInsP_3$). Also, in the absence of ultraviolet light, the ether linkage should be more resistant to metabolism or hydrolysis than the phosphodiester linkage previously used[14] to cage $InsP_3$.

$CmInsP_3$ was synthesized from *myo*-inositol in 14 steps, then esterified to produce $cmInsP_3$/PM (Fig. 2A). Binding of $cmInsP_3$ to the $InsP_3R$ (assayed by displacement of ^3H-labelled $InsP_3$) was negligible (<0.5% of binding of real $InsP_3$). However, ultraviolet illumination of $cmInsP_3$ progressively released material that bound tightly to the $InsP_3R$ (Fig. 2B). The product of exhaustive photolysis bound to the $InsP_3R$ equivalently to 75% of an equimolar amount of real $InsP_3$. Assuming that $mInsP_3$ was formed at 100% chemical yield, it is 75% as potent as $InsP_3$, making $mInsP_3$ the most potent synthetic $InsP_3$ analogue known[5]. The quantum yield of photolysis was 0.09 ± 0.013. At 365 nm, the uncaging cross-section of $cmInsP_3$, 450 M^{-1} cm^{-1}, slightly exceeded the 325 M^{-1} cm^{-1} reported for an earlier caged $InsP_3$, a $P^{4(5)}$-1-(2-nitrophenyl)ethyl ester[14].

Incubation of 1321N1 astrocytoma cells with 2 μM extracellular $cmInsP_3$/PM for 5, 30 and 60 min resulted in 33 ± 5, 201 ± 9 and 260 ± 10 pmol (mean ± s.e.m.), respectively, of trapped $cmInsP_3$, per million cells. The final values were equivalent to intracellular concentrations of hundreds of micromolar. The ability of $cmInsP_3$ to accumulate to a much higher concentration inside the cells than the concentration of $cmInsP_3$/PM outside the cells confirmed that $cmInsP_3$ was being trapped by irreversible ester hydrolysis, and implied that unphotolysed $cmInsP_3$ must be quite stable inside living cells. The trapped $cmInsP_3$ had no effect on $[Ca^{2+}]_c$ even after prolonged incubation, as monitored[15] by the calcium indicator Fluo-3. Subsequent brief exposure of the cells to ultraviolet light (345–355 nm) caused a sudden increase in $[Ca^{2+}]_c$ levels whether extracellular calcium was present or not (Fig. 3a,b), showing that calcium was released from internal stores. Ultraviolet illumination was ineffective if applied less than two minutes after application of $cmInsP_3$/PM, as would be expected from the time required for the ester to cross membranes and release $cmInsP_3$. We routinely allowed ⩾30 min to ensure complete de-esterification of $cmInsP_3$/PM after washing away excess ester. Once $cmInsP_3$ was loaded into cells, it remained well trapped and non-metabolized. At room temperature, an additional incubation time of 8 h in the dark had almost no effect on the size of the subsequent flash-induced $[Ca^{2+}]_c$ transient. Incubation for 8 h at 37 °C did weaken the response, but the amplitude could be restored by a roughly threefold increase in exposure to ultraviolet light, indicating that about one-third of the $cmInsP_3$ remained. Other control experiments with the same or more than ten times stronger ultraviolet light, in the absence or presence of 100 μM 4,5-dimethoxy-2-nitrobenzyl methyl ether as a control for DMNB photolysis byproducts gave no detectable rise in $[Ca^{2+}]_c$ levels, either in normal calcium-containing or in calcium-free medium, showing that the response was specific to $cmInsP_3$. $CmInsP_3$/PM behaved similarly in other cell lines, including HeLa cells, human embryonic kidney 293 cells, REF-52 fibroblasts, T84 colonic epithelial cells, RBL-2H3 rat basophilic leukaemia cells (see below), and P388D1 macrophage-like cells, so its biological efficacy seems to be fairly general, at least in cultured mammalian cells.

$[Ca^{2+}]_c$ signals are essential for the activation of lymphoid cells, a process involving gene expression, differentiation and proliferation[6]. Non-invasive loading of $cmInsP_3$/PM into cells allowed assessment of the effect of different temporal patterns of $InsP_3R$ activation on $[Ca^{2+}]_c$ signals and gene expression. We used activation of the NF-AT (nuclear factor of activated T cells) transcription factor complex in RBL-2H3 cells as a model system. Increased $[Ca^{2+}]_c$ stimulates calcineurin to dephosphorylate pre-existing cytosolic NF-AT proteins (NF-ATc), which then migrate into the nucleus, bind to nuclear proteins and NF-AT-response elements, and activate downstream genes. Although NF-AT was first characterized in lymphocytes as a crucial element in interleukin-2 gene expression[6], it is widespread in lymphoid cells, including RBL cells[7]. We assayed NF-AT-driven gene expression at the level of single cells, using a stably transfected reporter construct in which a trimer of NF-AT-response elements drove expression of the bacterial enzyme β-lactamase. β-Lactamase activity can be assayed with a newly developed membrane-permeant fluorogenic substrate, which becomes trapped in individual live cells. In the absence of β-lactamase, the cells fluoresce at 520 nm, whereas expression of the

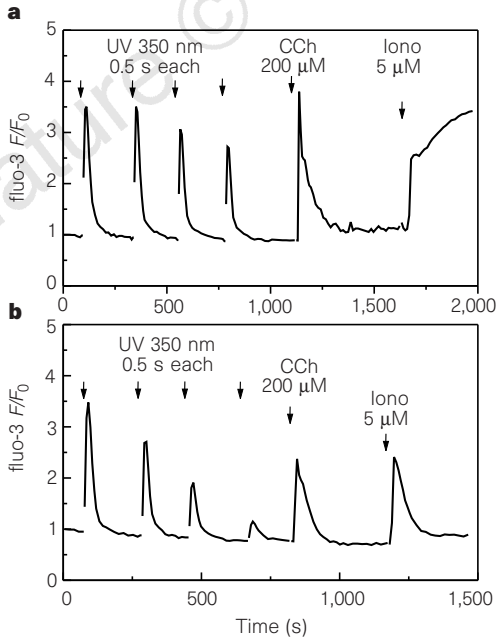

Figure 3 Cytosolic calcium transients evoked by photolysis of $cmInsP_3$ in 1321N1 astrocytoma cells. Transients were evoked in HBS medium containing normal levels of calcium (**a**) and in calcium-free DPBS saline containing 0.5 mM EGTA (**b**). UV 350 nm denotes uncaging flashes delivered through the microscope objective in which the excitation filter was switched for 0.5 s to a 345–355 nm bandpass. CCh, carbachol; Iono, ionomycin.

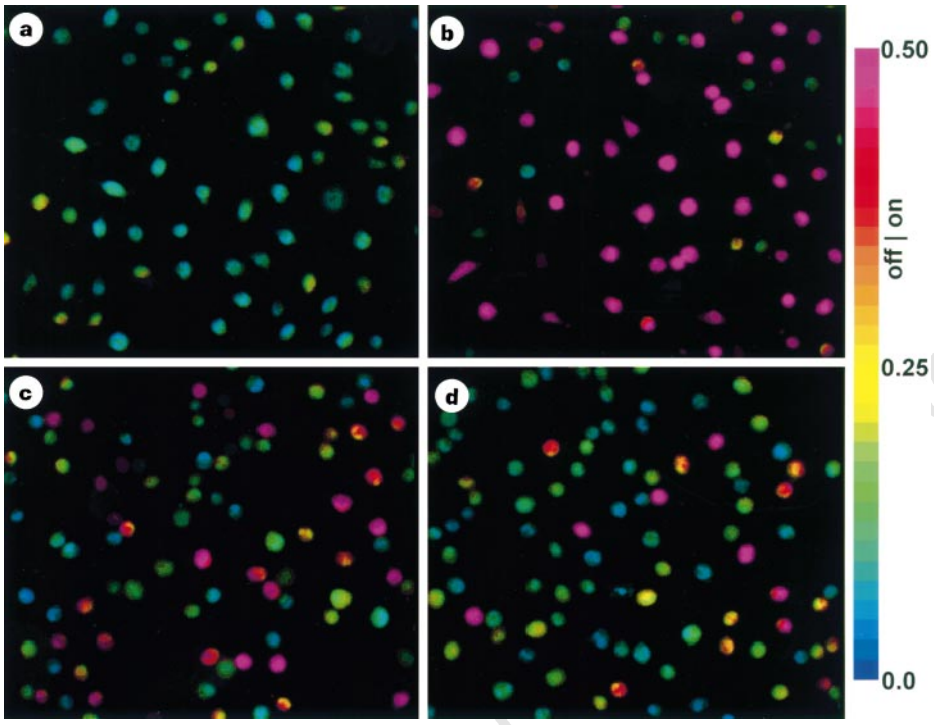

Figure 4 Expression of the β-lactamase reporter gene induced by uncaged cmInsP$_3$/PM. **a**, Unstimulated cells. **b**, Cells stimulated by 1 μM ionomycin for 20 min at 37 °C. **c**, **d**, Cells loaded with 10 μM cmInsP$_3$/PM were illuminated with four pulses each of ultraviolet light of 0.3, 0.6, 1 and 1.4 s duration, spaced 1 min (**c**) or 3 min (**d**) apart. The cells were then incubated for 3.5 h at 37 °C, and then stained for β-lactamase gene expression[16]. The ratio of 420–460 nm to 512–558 nm emissions while exciting at 392–408 nm is displayed in false colours calibrated by the colour scale at the right, which also indicates the threshold ratio (0.35) for a cell to be scored as positive for reporter gene expression.

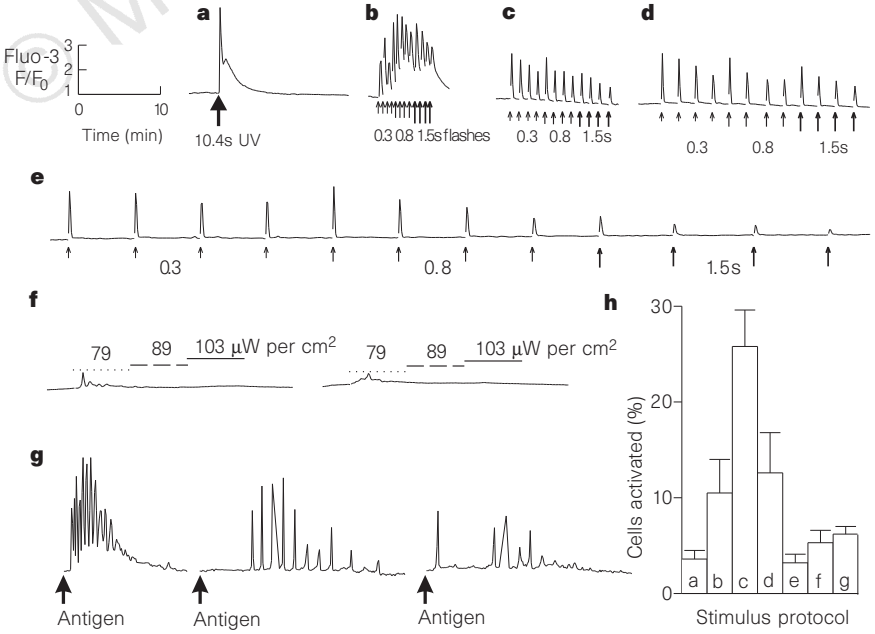

Figure 5 $[Ca^{2+}]_c$ levels measured by Fluo-3 fluorescence and NF-AT-driven β-lactamase gene expression evoked by different temporal patterns of photolysing the same total amount of cmInsP$_3$ in RBL cells. **a–g**, The time and Fluo-3 intensity scales at the upper left apply to all traces. **a**, 3.5×10^{-8} einstein·cm^{-2} s^{-1} or 11.4 mW cm^{-2} was delivered for 10.4 s where indicated. **b–e**, 12 Pulses of the same intensity were delivered in three groups of four flashes, each of 0.3, 0.8, and 1.5 s duration, spaced 30 s (**b**), 1 min (**c**), 2 min (**d**), and 8 min (**e**) apart. **f**, Continuous illumination with (2.42, 2.7, or 3.1) $\times 10^{-10}$ einstein·cm^{-2} s^{-1}, each for 7 min, represented by dotted, dashed, and solid lines, respectively. **g**, 50 ng ml^{-1} DNP-BSA was added at the point indicated by the arrow. Traces in **f**, **g** are from representative single cells, whereas traces in **a–e** are averages of 25 cells because the responses were much more homogeneous and synchronous. **g**, The average frequency of spikes of amplitude $\Delta F/F_0 > 0.5$ was 2.09, 0.66, and 0.39 min^{-1} at the left, centre and right, respectively. **h**, NF-AT-driven β-lactamase gene expression. Percentage of cells is shown with suprathreshold β-lactamase activity resulting from protocols **a–g**.

enzyme cleaves the substrate and changes the fluorescence maximum to 447 nm[16]. As this new reporter gene assay leaves the cells fully viable, we could use fluorescence-activated cell sorting to isolate a subclone of RBL cells in which NF-AT-driven gene expression was maximally responsive to sustained elevation of $[Ca^{2+}]_c$ levels. Figure 4 shows pseudocolour images of β-lactamase expression levels in this subclone under various stimulation conditions. Hues from blue to magenta indicate low to high levels of NF-AT-driven expression of β-lactamase, monitored by ratios of emissions at 447 nm and 520 nm. The responsiveness of NF-AT activity to $[Ca^{2+}]_c$ levels was shown by the contrast between the blue-green pseudocolour of unstimulated cells (Fig. 4a) and the predominant magenta pseudocolour of cells treated with a calcium ionophore (Fig. 4b). Uncaging of $cmInsP_3$ with 16 ultraviolet pulses spaced 1 min apart caused significant gene activation (a 3.5-fold increase in ratio, corresponding to a pseudocolour of orange or redder) in ~30% of the cells (Fig. 4c), whereas the same flashes spaced 3 min apart only activated ~10% of the cells (Fig. 4d).

To confirm and extend this preliminary finding of frequency selectivity, we used a wider variety of uncaging protocols and made parallel measurements of $[Ca^{2+}]_c$ in the experiments shown in Fig. 5. For Fig. 5a, the ultraviolet light was applied in a single pulse of 11.4 mW per cm^2 that lasted 10.4 s, enough to photolyse ~30% of the loaded $cmInsP_3$. This generated a big $[Ca^{2+}]_c$ spike, which gradually returned to the resting level in <5 min. For Fig. 5b–e, the same intensity of ultraviolet light was applied in four pulses of 0.3 s, then four pulses of 0.8 s, and finally four pulses of 1.5 s duration; flashes were spaced 30 s (Fig. 5b), 1 min (Fig. 5c), 2 min (Fig. 5d), or 8 min (Fig. 5e) apart. Each flash produced a separate synchronized $[Ca^{2+}]_c$ spike; the increasing durations in the second and third groups of four pulses acted to maintain roughly constant spike amplitudes. In Fig. 5f, dim continuous illumination of 79, 89 and 103 μW per cm^2 was applied for 7 min each, with no gaps. Each of the three 7-min episodes contained enough ultraviolet light to photolyse ~10% of the initial $cmInsP_3$. Even though the cumulative amount of $mInsP_3$ released in this protocol was similar to the amount of $mInsP_3$ released in the other protocols, and the overall duration of $mInsP_3$ release was intermediate between that of Fig. 5c and d, individual cells (for example, Fig. 5f) gave at most a few $[Ca^{2+}]_c$ transients, typically three to four, before subsiding. A roughly optimal dose of a relatively physiological agonist, surface immunoglobulin E crosslinked by dinitrophenylated albumin, evoked oscillations of extremely heterogeneous amplitude and frequency[17,18] (Fig. 5g). Figure 5h summarizes the gene expression resulting from these different protocols. The most effective protocol used 12 flashes spaced 1 min apart; this activated NF-AT in 26% of the cells. This protocol was almost as effective as maintaining elevated $[Ca^{2+}]_c$ levels for 15 min with a calcium ionophore; this activated 28% of the cells. Spacings of 0.5 min and 2 min were each about half as effective as spacings of 1 min. The single 10.4 s pulse, the 12 pulses spaced 8 min apart, and the dim continuous illumination for 21 min all activated NF-AT in only 3–5% of cells. When either the $cmInsP_3$/PM or the ultraviolet illumination, or both, were withheld, negligible activation (<1%) resulted. Antigen stimulation was only modestly effective (6%), perhaps because the heterogeneous calcium responses matched optimal patterns in only a small fraction of the cells.

These results indicate that one of the best defined signal-transduction cascades into the nucleus may be tuned to the frequency of $[Ca^{2+}]_c$ spikes. The single burst of $InsP_3$ or excessively frequent oscillations of $InsP_3$ (Fig. 5a, b) may have failed to maintain elevated $[Ca^{2+}]_c$ levels for enough time[19,20]. The lower-frequency oscillations (Fig. 5d,e) may have allowed too much time for rephosphorylation and nuclear exit of NF-ATc between pulses[19]. Slow, steady production of $InsP_3$ (Fig. 5f) was remarkably ineffective at increasing $[Ca^{2+}]_c$ levels for prolonged periods, perhaps because of $InsP_3R$ desensitization[21,22]. This observation may help to explain why cells generate oscillations in $[Ca^{2+}]_c$ and perhaps $InsP_3$ as well[2,18]. Cells might only be able to generate a limited total amount of $InsP_3$, because $InsP_3$ biosynthesis use many ATP molecules and depletes stores of the scarce lipid phosphatidylinositol-4,5-bisphosphate. Repetitive pulses (Fig. 5c) were much better than continuous dribbling of the same total amount of $InsP_3$ (Fig. 5f) for producing big and reliable $[Ca^{2+}]_c$ spikes, which in turn optimally activated at least one prototypic calcium-responsive transcription factor (see also ref. 8). Other genes[20] and cell functions[23] dependent on $InsP_3$ and $[Ca^{2+}]_c$ should also be investigated by this new, convenient method to activate the $InsP_3R$ under spatiotemporal control in large populations of fully intact cells. □

Methods

Synthesis of $cmInsP_3$ and $cmInsP_3$/PM. See Fig. 2A. Fast atom bombardment mass spectroscopy showed an exact mass for compound $\mathbf{1} + Cs^+$ of 1,305.1481 compared with 1,305.1444 calculated for $C_{41}H_{62}O_{32}NP_3 + Cs^+$. ^1H and ^{31}P magnetic resonance spectra were also satisfactory.

Determination of the photolysis quantum yield of $cmInsP_3$ and affinity of binding of $mInsP_3$ to the $InsP_3R$. 1 μM $cmInsP_3$ in Hanks' balanced salts (HBS) buffer plus 1 mg ml^{-1} bovine serum albumin and 2 mM 2-mercaptoethanol was photolysed at 365 nm at 0 °C. Binding of $mInsP_3$ to the $InsP_3R$ was measured ($InsP_3$ assay kit, Amersham) at the indicated times. The quantum yield, Q, of the photolysis was calculated from the exponential progress curve the extinction coefficient (5×10^6 cm^2 mol^{-1}) of $cmInsP_3$ at 365 nm, and the ultraviolet intensity (1.41×10^{-8} einstein·cm^2 s^{-1}) measured by ferrioxalate actinometry[24].

Determination of loading efficiency of $cmInsP_3$/PM. Confluent monolayers of astrocytoma cells in 35-mm tissue culture dishes were incubated with 2 μM $cmInsP_3$/PM for the indicated time. After washing and 30 min incubation, the saline was aspirated and the cells were quenched with 0.5 ml ice-cold perchloric acid containing 2 mM EDTA and 20 mM HEPES. The $cmInsP_3$ was then thoroughly photolysed at 0 °C with 365 nm ultraviolet light. The samples were neutralized with KOH, centrifuged to remove $KClO_4$, and assayed for $InsP_3$ normalized to the number of cells. Experiments were done in duplicate on separate dishes of cells.

Monitoring cytosolic Ca^{2+} transients produced by uncaging $cmInsP_3$. 1321N1 astrocytoma cells were loaded with $cmInsP_3$/PM (2 μM) and Fluo-3/AM (2 μM) in HBS containing 0.05% Pluronic F-127 for 1 h at room temperature. Cells were then washed and incubated for another 30 min. Fluo-3 intensity[15] (F, 480 ± 15 nm excitation, 535 ± 22.5 nm emission) was monitored every 7 s by digital-imaging microscopy and was plotted, after background subtraction, as a ratio against the Fluo-3 intensity at the resting calcium level (F_0). Ultraviolet pulses for the experiments of Fig. 3 were from a 150 W xenon arc, attenuated by a neutral density filter of 4% nominal transmission, filtered by a 345–355 nm bandpass filter, and delivered through a ×40/1.3 NA oil-immersion objective. Typically, at least 13 cells were averaged, and the results shown are representative of three experiments. The same procedure was used for the RBL cells transfected with the reporter gene, except that the $cmInsP_3$/PM and Fluo-3/AM concentrations were 6 μM and 1 μM, respectively, 365 nm ultraviolet light was delivered to the entire dish of cells from a mercury lamp clamped above the stage of the inverted microscope, and the $[Ca^{2+}]_c$ responses of at least 25 cells were averaged. The short uncaging pulses of 11.4 mW per cm^2 or 3.5×10^{-8} einstein·cm^{-2} s^{-1} were gated by an electronic shutter. The $[Ca^{2+}]_c$ traces shown were obtained at room temperature. Responses at 37 °C to uncaging pulses were essentially the same as shown, and the asynchronous oscillations in response to the continuous illumination lasted a few more cycles but still terminated well before the end of the first 7 min of exposure to ultraviolet light.

Generation of an RBL cell line stably incorporating the NF-AT–β-lactamase transcriptional reporter. The pZeo–NF-AT–BLA vector was constructed by cloning a trimer of NF-AT-response-element promoters[25] upstream of a cytoplasmic form of β-lactamase[16]. This construct was made using the pZeoSV (Invitrogen) expression vector minus its SV40 promoter. RBL-2H3 cells were transfected by electroporation with pZeo–NF-AT–BLA DNA and selected in RPMI-1640 medium with 10% fetal bovine serum and 250 μg ml^{-1} zeocin for 2 weeks. The stably transfected population of RBL cells was

subcloned by stimulating with 1 μM ionomycin for 3 h, vital staining with the membrane-permeant β-lactamase substrate CCF2/AM[16], and fluorescence-activated cell sorting. The best clone gave 95–100% β-lactamase-positive cells with such stimulation and was used for all the subsequent studies on RBL cells.

Uncaging cmInsP$_3$ and measurement of reporter gene expression. The RBL cells were loaded with 10 μM cmInsP$_3$/PM for 30 min (Fig. 4) or with 6 μM ester for 1 h (Fig. 5h), and were then incubated in ester-free medium for 0.5 h at room temperature. Uncaging of cmInsP$_3$ was performed at 37 °C in culture medium in a sealed thermostated perfusion chamber (Bioptechs, Butler, PA) with the same shuttered mercury lamp as for the $[Ca^{2+}]_c$ measurements. The cells were left for 3.5 h at 37 °C, loaded for 30 min at room temperature with 5 μM of the β-lactamase substrate CCF2/AM in HBS containing 0.05% Pluronic F-127, and finally washed and incubated for 30 min at room temperature. β-Lactamase expression was scored by exciting at 392–408 nm wavelength and viewing the ratio of 420–460 to 512–558 nm emissions[16]. A charge-coupled-device camera (Photometrics) and ratio-imaging software (Metafluor, Universal Imaging) were used to obtain the data shown in Fig. 4 and to score borderline cells for Fig. 5h. Cells whose 420–460 nm to 512–558 nm ratio was >0.35, that is, 2.3 times that of control non-stimulated cells, were counted as activated. Over 200 cells were counted for each experiment, and the data shown in Fig. 5h are averages of three separate experiments. Over 1,200 cells were counted for each stimulation condition shown in Fig. 4.

Control stimuli for gene expression. For exposures to ultraviolet light in the absence of cmInsP$_3$/PM, we used the uncaging protocols of Fig. 5b or Fig. 5c. Ionomycin (1 μM) treatments at 37 °C were terminated by washing with fresh medium containing 5 mg ml^{-1} bovine serum albumin to sequester the ionophore. The cells were then incubated with 1.3 mM Ca^{2+} (Fig. 4b) or 3 mM EGTA. In the latter case, 15 and 30 min incubations with ionophore activated β-lactamase in 28 ± 5 and 65 ± 9% of the cells, respectively. To stimulate with antigen, the RBL cells were passively sensitized for 12 h with monoclonal murine IgE antibodies against dinitrophenyl (DNP) (Sigma). The cells were washed five times with fresh medium and incubated at 37 °C for 45 min before antigen stimulation. Dinitrophenylated bovine serum albumin (DNP-BSA, Calbiochem) was added at a final concentration of 50 or 500 ng ml^{-1}. 50 ng ml^{-1} DNP-BSA caused the highest degree (in both amplitude and duration) of intracellular calcium mobilization, though the calcium transients in individual cells were heterogenous. 500 ng ml^{-1} DNP-BSA caused negligible mobilization of intracellular calcium and activated β-lactamase in only 2.1 ± 0.9% of cells.

Received 5 December 1997; accepted 6 March 1998.

1. Berridge, M. J. Inositol triphosphate and calcium signalling. *Nature* **361,** 315–325 (1993).
2. Tsien, R. W. & Tsien, R. Y. Calcium channels, stores, and oscillations. *Annu. Rev. Cell Biol.* **6,** 715–760 (1990).
3. Jacob. R. Calcium oscillations in electrically nonexcitable cells. *Biochim. Biophys. Acta* **1052,** 427–438 (1900).
4. Fewtrell, C. Ca^{2+} oscillations in non-excitable cells. *Annu. Rev. Physiol.* **55,** 427–454 (1993).
5. Potter, B. V. L. & Lampe, D. Chemistry of inositol lipid mediated cellular signaling. *Angew. Chemie Int. Edn Engl.* **34,** 1933–1972 (1995).
6. Crabtree, G. R. & Clipstone, N. A. Signal transmission between the plasma membrane and nucleus of T lymphocytes. *Annu. Rev. Biochem.* **63,** 1045–1083 (1994).
7. Hutchinson, L. E. & McCloskey, M. A. FcεRI-mediated induction of nuclear factor of activated T-cells. *J. Biol. Chem.* **270,** 16333–16338 (1995).
8. Dolmetsch, R. E., Xu, K. & Lewis, R. S. Calcium oscillations increase the efficacy and specificity of gene expression. *Nature* **392,** 933–936 (1998).
9. Hirata, M. *et al*. Stereospecific recognition of inositol 1,4,5-triphosphate analogs by the phosphatase, kinase, and binding proteins. *J. Biol. Chem.* **265,** 8404–8407 (1990).
10. Hirata, M., Watanabe, Y., Yoshida, M., Koga, T. & Ozaki, S. Roles for hydroxyl groups of D-myo-inositol 1,4,5-triphosphate in the recognition by its receptor and metabolic enzymes. *J. Biol. Chem.* **268,** 19260–19266 (1993).
11. Kozikowski, A. P., Ognyanov, V. I., Fauq, A. H., Nahorski, S. R. & Wilcox, R. A. Synthesis of 1D-3-deoxy-, 1D-2,3-dideoxy-, and 1D-2,3,6-trideoxy-*myo*-inositol 1,4,5-trisphosphate from quebrachitol, their binding affinities, and calcium release activity. *J. Am. Chem. Soc.* **115,** 4429–4434 (1993).
12. Li, W.-h., Schultz, C., Llopis, J. & Tsien, R. Y. Membrane-permeant esters of inositol polyphosphates, chemical synthesis and biological applications. *Tetrahedron* **53,** 12017–12040 (1997).
13. Adams, S. R. & Tsien, R. Y. Controlling cell chemistry with caged compounds. *Annu. Rev. Physiol.* **55,** 755–784 (1993).
14. Walker, J. W., Feeney, J. & Trentham, D. R. Photolabile precursors of inositol phosphates. Preparation and properties of 1-(2-nitrophenyl)ethyl esters of *myo*-inositol 1,4,5-trisphosphate. *Biochemistry* **28,** 3272–3280 (1989).
15. Kao, J. P. Y., Harootunian, A. T. & Tsien, R. Y. Photochemically generated cytosolic calcium pulses and their detection by fluo-3. *J. Biol. Chem.* **264,** 8179–8184 (1989).
16. Zlokarnik, G. *et al*. Quantitation of transcription and clonal selection of single living cells with β-lactamase as reporter. *Science* **279,** 84–88 (1998).
17. Kuchtey, J. & Fewtrell, C. Subcloning of RBL-2H3 mucosal mast cell line reduces Ca^{2+} response heterogeneity as the single-cell level. *J. Cell. Physiol.* **166,** 643–652 (1996).
18. Smith, G. D., Lee, R. J., Oliver, J. M. & Keizer, J. Effect of Ca^{2+} influx on intracellular free Ca^{2+} responses in antigen-stimulated RBL-2H3 cells. *Am. J. Physiol.* **270,** C939–C952 (1996).
19. Timmerman, L. A., Clipstone, N. A., Ho, S. N., Northrop, J. P. & Crabtree, G. R. Rapid shuttling of NF-AT in discrimination of Ca^{2+} signals and immunosuppression. *Nature* **383,** 837–840 (1996).
20. Dolmetsch, R. E., Lewis, R. S., Goodnow, C. G. & Healy, J. I. Differential activation of transcription factors induced by Ca^{2+} response amplitude and duration. *Nature* **386,** 855–858 (1997).
21. Hajnóczky, G. & Thomas, A. P. The inositol trisphosphate calcium channel is inactivated by inositol trisphosphate. *Nature* **370,** 474–477 (1994).
22. Oancea, E. & Meyer, T. Reversible desensitization of inositol trisphosphate-induced calcium release provides a mechanism for repetitive calcium spikes. *J. Biol. Chem.* **271** 17253–17260 (1996).
23. Gu, X. & Spitzer, N. C. Distinct aspects of neuronal differentiation encoded by frequency of spontaneous Ca^{2+} transients. *Nature* **375,** 784–787 (1995).
24. Hatchard, C. G. & Parker, C. A. A new sensitive chemical actinometer. II. Potassium ferrioxalate as a standard chemical actinometer. *Proc. R. Soc. Lond. A* **235,** 518–536 (1956).
25. Fiering, S. *et al*. Single cell assay of a transcription factor reveals a threshold in transcription activated by signals emanating from the T-cell antigen receptor. *Genes Dev.* **4,** 1823–1834 (1990).
26. Vacca, J. P. *et al*. The total synthesis of myo-inositol polyphosphates. *Tetrahedron* **45,** 5679–5702 (1989).

Acknowledgements. We thank E. A. Dennis for loan of facilities and S. R. Adams, A. Miyawaki, T. J. Rink and P. A. Negulescu for advice. This work was funded by the NIH and HHMI.

Correspondence and requests for materials should be addressed to R.Y.T.

NMR structure and mutagenesis of the FADD (Mort1) death-effector domain

Matthias Eberstadt, Baohua Huang, Zehan Chen, Robert P. Meadows, Shi-Chung Ng, Lixin Zheng*, Michael J. Lenardo* & Stephen W. Fesik

Pharmaceutical Discovery Division, Abbott Laboratories, Abbott Park, Illinois 60064, USA

** Laboratory of Immunology, National Institutes of Health, Bethesda, Maryland 20892, USA*

When activated, membrane-bound receptors for Fas and tumour-necrosis factor initiate programmed cell death by recruiting the death domain of the adaptor protein FADD[1] (Mort1; ref. 2) to the membrane. FADD then activates caspase 8 (ref. 3) (also known as FLICE[4] or MACH[5]) through an interaction between the death-effector domains of FADD and caspase 8. This ultimately leads to the apoptotic response. Death-effector domains and homologous protein modules known as caspase-recruitment domains[6] have been found in several proteins[1–14] and are important regulators of caspase (FLICE) activity and of apoptosis. Here we describe the solution structure of a soluble, biologically active mutant of the FADD death-effector domain. The structure consists of six anti-parallel, amphipathic α-helices and resembles the overall fold of the death domains of Fas[15] and p75 (ref. 16). Despite this structural similarity, mutations that inhibit protein–protein interactions involving the Fas death domain have no effect when introduced into the FADD death-effector domain. Instead, a hydrophobic region of the FADD death-effector domain that is not present in the death domains is vital for binding to FLICE and for apoptotic activity.

As neither the wild-type death-effector domain (DED) of FADD nor full-length FADD could be obtained in a form that was suitable for study by nuclear magnetic resonance (NMR), we prepared several site-directed mutants and screened them for their ability to be expressed as a soluble protein, induce apoptosis and bind to FLICE. On the basis of its high solubility in a monomeric form (0.7 mM) and wild-type-like biological activities (Fig. 1), we chose the Phe 25 → Tyr (F25Y) mutant protein for structure determination.

The structure of the F25Y FADD DED is well defined by the 1,102 experimentally derived NMR restraints (Fig. 2a) and consists of six antiparallel, amphipathic α-helices (Fig. 2b). The α-helices are